



ELSEVIER

Biochimica et Biophysica Acta 1506 (2001) 31–46



www.bba-direct.com

Fluorescent probes for non-invasive bioenergetic studies of whole cyanobacterial cells

Markus Teuber, Matthias Rögner, Stephan Berry *

Lehrstuhl Biochemie der Pflanzen, Ruhr-Universität Bochum, D-44780 Bochum, Germany

Received 29 January 2001; received in revised form 19 March 2001; accepted 27 March 2001

Abstract

Fluorescent ΔpH and $\Delta\Psi$ indicators have been screened for the non-invasive monitoring of bioenergetic processes in whole cells of the cyanobacterium *Synechocystis* sp. PCC 6803. Acridine yellow and Acridine orange proved to be the best ΔpH indicators for the investigation of thylakoid and cytoplasmic membrane energization: While Acridine yellow indicated only cytosolic energization, Acridine orange showed signals from both the thylakoid lumen and the cytosol that could be separated kinetically. Both indicators were applied successfully to monitor cellular energetics, such as the interplay of linear and cyclic photosynthetic electron transport, osmotic adaptation and solute transport across the cytoplasmic membrane. In contrast, useful membrane potential indicators were more difficult to find, with Di-4-ANEPPS and Brilliant cresyl blue being the only promising candidates for further studies. Finally, Acridine yellow and Acridine orange could also be applied successfully for the thermophilic cyanobacterium *Synechococcus elongatus*. Different from *Synechocystis* sp. PCC 6803, where both respiration and ATP hydrolysis could be utilized for cytoplasmic membrane energization, proton extrusion at the cytoplasmic membrane in *Synechococcus elongatus* was preferentially driven by ATP hydrolysis. © 2001 Elsevier Science B.V. All rights reserved.

Keywords: Indicator dye; Membrane potential; Proton translocation; Transport process; *Synechococcus elongatus*; *Synechocystis* sp. PCC 6803

Abbreviations: CCCP, carbonylcyanide-3-chlorophenyl hydrazone; Chl, chlorophyll; CM, cytoplasmic membrane; DBMIB, 2,5-dibromo-3-methyl-6-isopropyl-*p*-benzoquinone; DCCD, *N,N'*-dicyclohexyl-carbodiimide; DCMU, 3-(3,4-dichlorophenyl)-1,1-dimethylurea; DSPD, *N,N'*-disalicylidene-1,3-propanediamine; Fd, ferredoxin; Fecy, 'ferricyanide' ($\text{K}_3[\text{Fe}(\text{CN})_6]$); FNR, ferredoxin:NADP oxidoreductase; FRL, far red light; MV, methyl viologen; NDH, NAD(P)H dehydrogenase; PS I, Photosystem I; PS II, Photosystem II; RL, red light; *Synechocystis* 6803, *Synechocystis* sp. PCC 6803; TTFA, 1-(2-thenoyl)-3,3,3-trifluoroacetone; WT, wild type; $\Delta F/F_0$, relative change of indicator fluorescence; $\Delta\Psi$, electrical potential difference across membranes; For abbreviations of dye names see Table 1

* Corresponding author. Fax: +49-234-321-4322; E-mail: stephan.berry@ruhr-uni-bochum.de

1. Introduction

A large number of fluorescent indicators for both ΔpH and $\Delta\Psi$ measurements across biological membranes are available [1–3]. Although there are alternative methods, such as the use of radioactive [4–11] or spin-labeled probes [1,12], they require more experimental effort and, in particular in the case of radioactive probes, the time resolution of the method is lower. Targeted expression of pH-sensitive variants of the green fluorescent protein (GFP) is another elegant method for determining intracellular pH [13], but the method is time-consuming as for each strain under investigation, the corresponding GFP-

expressing mutant has first to be created. In summary, bioenergetic fluorescence measurement combines the advantages of an easy performance and a good time resolution.

Using fluorescent dyes, various systems such as membrane vesicle preparations, spheroplasts or whole cells from different phototrophic organisms have been investigated [9,10,14–24]. However, reports on intact cyanobacterial cells are comparatively rare, especially with respect to light-induced changes of cellular energization [25–27]; for the two organisms investigated in the present paper, we are aware of only one such study with *Synechocystis* 6803 [28] and none with *Synechococcus elongatus*.

Cyanobacterial cells pose problems for bioenergetic studies because there are three compartments (cytosol, thylakoid lumen and periplasm/cell surroundings) to be considered. In some cases, in particular in *Synechocystis* 6803, there may be also difficulties with respect to dye uptake into the cell. Nevertheless, intact cells as a study object have a major advantage compared to vesicle preparations: There will be no preparation artifacts and the interplay of different processes at the cellular level can be monitored. The two organisms used in this study were selected due to their importance in photosynthesis research: *Synechocystis* 6803 is popular for genetic studies as it is easily transformable and its whole genomic sequence is known [29]; it is often considered as a model organism for the study of oxygenic photosynthesis. *Synechococcus elongatus* is likely to become similarly important in the future, as its complete genome sequence will be available soon (S. Tabata, personal communication) and, being a thermophile, it is a source for stable proteins, which can be successfully crystallized and used for X-ray analysis, as demonstrated both for PS I [30] and PS II [31].

In the present study, we investigated light-induced changes of membrane energization and the different processes involved: photosynthesis vs. respiration, linear vs. cyclic photosynthetic electron transport, and transport processes at the CM. The strategy consisted of two steps:

1. Screening for suitable indicators using *Synechocystis* 6803
2. Characterization of the signals from the most

promising dyes and the bioenergetic reactions indicated by them. In order to deconvolute the various processes at the cytoplasmic and thylakoid membrane, different inhibitors and mutant strains of *Synechocystis* 6803 have been used, which were lacking different bioenergetic protein complexes. A preliminary characterization indicated that methods, which were optimized for *Synechocystis* 6803, can also be applied successfully for *Synechococcus elongatus*

2. Materials and methods

2.1. Strains and culture conditions

Cells of *Synechocystis* 6803 were cultivated at a light intensity of $50 \mu\text{E m}^{-2} \text{s}^{-1}$ for 5 days in BG-11 medium at 30°C under aerobic conditions in Erlenmeyer flasks with 10 mM glucose. Besides WT, the following *Synechocystis* 6803 mutant strains were used: $\Delta\text{PS I}$ ($=\text{psaAB}^-$) [32], $\Delta\text{PS II}$ ($=\text{psbB}^-$) [33], $3 \times \Delta\text{Ox}$ ($=\text{ctaDIEI}^-/\text{ctaDIIIEII}^-/\text{cydAB}^-$) [34], $3 \times \Delta\text{Ox}\Delta\text{PS II}$ ($=\text{ctaDIEI}^-/\text{ctaDIIIEII}^-/\text{cydAB}^-/\text{psbB}^-$) (C.A. Howitt, W.F.J. Vermaas, personal communication), PAL ($=\text{apcAB}^-/\text{lapcE}^-/\text{lcm}^-$) [35] and M55 ($=\text{ndhB}^-$) [36]. Cultivation of the mutant strains was identical to WT, except for $\Delta\text{PS I}$ (growth at $5 \mu\text{E m}^{-2} \text{s}^{-1}$ with 30 mM glucose) and M55 (growth at $20 \mu\text{E m}^{-2} \text{s}^{-1}$ in a 300-ml airlift fermenter, aerated with air+5% CO_2). Cells of *Synechococcus elongatus* were grown for 7 days in DNT medium at a light intensity of $40 \mu\text{E m}^{-2} \text{s}^{-1}$ and at 55°C , using a 300 ml airlift fermenter (air enriched with 5% CO_2).

2.2. Indicator dyes

All dyes were bought in the highest available purity and used without further purification, except for Acriflavine and Proflavine, which are commercially available as a 65:35% mixture and which were separated by column chromatography (silica gel with cyclohexane/ethyl acetate/acetic acid = 4:2:0.01 as mobile phase). Stock solutions of the dyes (2 mM in DMSO) were stored at -20°C . Absorption and fluorescence spectra of the dyes (at $50 \mu\text{M}$ in BG-11 medium) were recorded with a Beckman DU 7400

Spectrophotometer and a SLM-Aminco Series 2 luminescence spectrometer (slit width 4 nm for excitation and detection), respectively. The maximum wavelengths for excitation and emission are given in Table 1.

2.3. Measurement protocols

Time-resolved measurements of indicator fluorescence with cells at 30°C (all *Synechocystis* 6803 strains) or 55°C (*Synechococcus elongatus*) were done in a laboratory-built setup. The measurements were based on the Lock-In technique, using a pulsed light source for dye excitation (LEDs for excitation above 400 nm; a halogen lamp with a light chopper for excitation below 400 nm). In both cases, the light source was equipped with bandpass filters (Schott DAL or Omega BP8). Excitation and detection of indicator fluorescence was done by a branched fiber-optics. The detector was a photomultiplier, protected by appropriate filters (Schott DAL or Omega BP8, Balzers DT Blue or DT Cyan). To avoid a high background of phycobilisome or chlorophyll fluorescence, indicator fluorescence was recorded below 575 nm, even when the emission maximum of the dye was at a higher wavelength; in the phycobilisomeless PAL mutant detection at higher wavelengths was possible. The light intensity for dye excitation was sufficiently low to avoid actinic effects. Unless indicated, routinely an indicator concentration of 5 μM and a chlorophyll *a* concentration of about 15 μM were used. The cell suspension was supplemented with 50 mM TRICIN/pH 8 before measurements. Two types of experiments were performed:

1. Kinetics of indicator uptake into the cells in the dark. In this case, the dye was added to the cells at the beginning of the measurement
2. Detection of light-induced changes of indicator fluorescence. In this case, the cells were incubated with the indicator in the dark for 20 min before the measurement

The source for actinic light was a halogen lamp with filters for red light ('RL', 4 mm Schott RG 630+Balzers Calflex-3000) or far red light ('FRL', 3 mm Schott RG 695+2 mm Schott RG 715+Balzers Calflex-3000). Oxygen evolution of *Synechocystis*

6803 WT cells during saturating red illumination was measured with a Clark-type oxygen electrode (Hansatech, UK) at 30°C in BG-11 medium supplemented by 10 mM NaHCO_3 .

2.4. Interpretation of the light-induced fluorescence changes of ΔpH indicating amines

For ΔpH indicating fluorescent amines, a simple relation between fluorescence quenching and the ΔpH across the thylakoid membrane has been proposed [16], based on the assumption that luminal enrichment of the protonated amine is the only cause of fluorescence quenching. However, the crucial step causing fluorescence quenching is the binding of the protonated amine to membrane lipids [17,37]. Further complications arise because both neutral and protonated forms of the amine are membrane permeable, and because several of the amines additionally undergo dimerization, which also affects fluorescence yield. Mathematical models taking all these processes into account are complex even for isolated thylakoids [17,23]. We thus did not apply such calculations on whole cells, where the situation is further complicated by the existence of two intracellular compartments and by unspecific indicator binding to DNA and proteins, and used the signals of fluorescent amines only as a semiquantitative indication of ΔpH changes. Averages of fluorescence signals from multiple determinations are presented as 'average \pm standard deviation (number of experiments)'.

3. Results and discussion

3.1. Screening of ΔpH indicators in *Synechocystis* 6803

Table 1 and Fig. 1 show all fluorescence probes used in this study. For measurements with cyanobacterial cells, a dye should meet several criteria:

1. Absorption and emission should be between 400 and 600 nm to minimize problems caused by the autofluorescence of the cells
2. Fluorescence yield should be high
3. There should be no undesired side effects of the dye as an inhibitor or uncoupler

Table 1
Indicator dyes for detection of ΔpH and $\Delta\Psi$

Substance class	Name; acronym (CI number)	Structure ^a	Wavelength (nm)		Use ^b	Source	Refs.	
			Excitation	Emission				
1-Amino-naphthalenes	<i>N</i> -(1-Naphthyl)-ethylenediamine; NED	1	$\text{R}^1 = \text{CH}_2\text{CH}_2\text{NH}_2$ $\text{R}^2 = \text{H}$	325	430	ΔpH	Fluka	[16,24,37]
	8-Anilino-naphthalene-1-sulfonic acid; ANS	1	$\text{R}^1 = \text{C}_6\text{H}_5$ $\text{R}^2 = \text{SO}_3\text{H}$	360	540	$\Delta\Psi$	Fluka	[9,10]
9-Amino-acridines	9-Aminoacridine; 9-AA	2	$\text{R}^1 = \text{R}^2 = \text{R}^3 = \text{H}$	400	455	ΔpH	Aldrich	[5,10,16,17,22, 23,25,37]
	9-Amino-6-chloro-2-methoxyacridine; ACMA	2	$\text{R}^1 = \text{H}$ $\text{R}^2 = \text{Cl}$ $\text{R}^3 = \text{CH}_3\text{O}$	411	496	ΔpH	Sigma	[17,20,27,28]
	Quinacrine; QA	2	$\text{R}^1 = \text{CH}(\text{CH}_3)-(\text{CH}_2)_3-$ $\text{N}(\text{C}_2\text{H}_5)_2$ $\text{R}^2 = \text{Cl}$ $\text{R}^3 = \text{CH}_3\text{O}$	422	503	ΔpH	Fluka	[10,14,17,22]
3,6-Diamino-acridines	Rivanol	2	$\text{R}^1 = \text{H}$ $\text{R}^2 = \text{NH}_2$ $\text{R}^3 = \text{C}_2\text{H}_5\text{O}$	420 ^e	511	$\Delta\text{pH}?$	Aldrich	
	Proflavine	3	$\text{R}^1 = \text{R}^2 = \text{H}$	452	512	$\Delta\text{pH}?$	Fluka	
	Acridine yellow; AY (CI 46025)	3	$\text{R}^1 = \text{CH}_3$ $\text{R}^2 = \text{H}$	445	510	$\Delta\text{pH}?$	Aldrich	
Xanthenes	Acridine orange; AO (CI 46005)	3	$\text{R}^1 = \text{H}$ $\text{R}^2 = \text{CH}_3$	493	531	ΔpH	Sigma	[19]
	Acridine orange; AO (CI 46005)	3	$\text{R}^1 = \text{H}$ $\text{R}^2 = \text{CH}_3$	493	531	ΔpH	Sigma	[19]
	Acridine orange; AO (CI 46005)	3	$\text{R}^1 = \text{H}$ $\text{R}^2 = \text{CH}_3$	493	531	ΔpH	Sigma	[19]
	Acriflavine (CI 46000)	4		466	508	$\Delta\text{pH}?$	Fluka	
	Pyronin G (CI 45005)	5	$\text{R} = \text{H}$	547	569	$\Delta\Psi$	Aldrich	[51]
	Tetramethyl rosamine; TMROS	5	$\text{R} = \text{C}_6\text{H}_5$	555	581	$\Delta\Psi$	Mol. Probes	[2]
	Rhodamine 123; R123	6	$\text{R}^1 = \text{NH}_2$ $\text{R}^2 = \text{H}$ $\text{R}_3 = \text{CH}_3$	500	527	$\Delta\Psi$	Acros	[26]
	Rhodamine 6G; R6G (CI 45160)	6	$\text{R}^1 = \text{NHC}_2\text{H}_5$ $\text{R}^2 = \text{CH}_3$ $\text{R}^3 = \text{C}_2\text{H}_5$	530	557	$\Delta\Psi$	Acros	[50]
Tetramethyl rhodamine methylester; TMRM	6	$\text{R}^1 = \text{N}(\text{CH}_3)_2$ $\text{R}^2 = \text{H}$ $\text{R}^3 = \text{CH}_3$	553	585	$\Delta\Psi$	Fluka	[50]	
Azines	Fluorescein diacetate; FDA (CI 45350)	7 ^d		443/pH 4 ^d 490/pH10 ^d	518/pH 4 and 10 ^d	ΔpH	Acros	[22,40]
	Phenosafranin (CI 50240)	8		520	593	$\Delta\Psi$	Aldrich	[53]
	Brilliant cresyl blue (CI 51010)	9		623	650	$\Delta\Psi?$	Aldrich	
Oxazines	Nile red (CI 51180)	10		585	664	$\Delta\Psi?$	Fluka	
	Auramine O (CI 41000)	11		450 ^e	505 ^e	$\Delta\Psi$	Aldrich	[15]
	Fuchsin (CI 42500)	12		565 ^e	595 ^e	$\Delta\Psi?$	Merck	
Isoquinolinium alkaloids	Berberine (CI 75160)	13		347	570	$\Delta\Psi$	Sigma	[55]
	Sanguinarine	14		470	605	$\Delta\Psi?$	Fluka	
Carbocyanines	DiIC18(3)	15	$\text{X} = \text{C}(\text{CH}_3)_2$ $\text{R} = \text{C}_{18}\text{H}_{37}$	568	595	$\Delta\Psi$	Fluka	[54]
	DiOC2(3)	15	$\text{X} = \text{O}$ $\text{R} = \text{C}_2\text{H}_5$	477	500	$\Delta\Psi$	Fluka	[54]
	DiSC8(3)	15	$\text{X} = \text{S}$ $\text{R} = \text{C}_8\text{H}_{17}$	557 ^f	571 ^f	$\Delta\Psi$	Fluka	[54]

Table 1
Indicator dyes for detection of ΔpH and $\Delta\Psi$

Substance class	Name; acronym (CI number)	Structure ^a	Wavelength (nm)		Use ^b	Source	Refs.
			Excitation	Emission			
Styryl dyes	Di-4-ANEPPS	16	510 ^g	600 ^g	$\Delta\Psi$	Biotium	[56]
	Oxonol VI	17	578	629	$\Delta\Psi$	Mol. Probes	[18,21]
	Oxonol 595	18	575	626	$\Delta\Psi$	Aldrich	

^aSee Fig. 1.

^bSubstances that have not previously been described in the literature for the respective application are marked by “?”.

^cMaximum absorption at 368 nm, but second peak at 420 is better suited for use with whole cells.

^dRefers to fluorescein instead of FDA.

^eMeasured in glycerol.

^fMeasured in pure water.

^gMeasured in cell suspension of *Synechocystis* 6803.

4. Unspecific binding to proteins, nucleic acids or membrane lipids should be low
5. The redox state of the dye should be stable, since the excited form especially of PS I is a strong reductant

Although some predictions on the behavior of the dye can be made based on its structure, it is impossible to assess all criteria in a purely theoretical way; therefore, a range of dyes was screened empirically to find the best candidates. These dyes came from three sources: reports on photosynthesis, on membrane biophysics (mitochondrial research, electrophysiology), and dyes that might be suited due to structural considerations, but which had not yet been used for monitoring ΔpH or $\Delta\Psi$.

The amine fluorescence method [14,16] is based on the decrease of the fluorescence yield of certain amines, in parallel with a decrease of the pH in the thylakoid lumen. Fig. 2a shows quenching of the 9-AA fluorescence during actinic illumination of *Synechocystis* 6803 cells. Different from this response, the 9-AA derivatives ACMA and QA showed a decrease during the illumination, which was followed by an increase (Fig. 2b,c): This multiphasic behavior is due to the concomitant processes of luminal acidification and cytosolic alkalization during illumination of cyanobacterial cells, as reported earlier for 9-AA and ACMA with *Plectonema boryanum* [25,27] and *Synechocystis* 6803 [28].

Light-induced pH changes in whole cells of various cyanobacterial species have also been investigated using alternative methods, such as distribution of spin-labeled [12] or radioactive probes [4,5,7], or measuring the pH-dependent NMR signals of ³¹P [38]. The major disadvantage of these methods is that they do not allow to directly monitor the different kinetic phases, as can be observed using fluorescent dyes (as shown in Fig. 2). Nevertheless, these data clearly indicate a general pattern in all species investigated: the cytoplasmic pH increases by about 0.5 units, while the lumen pH decreases by the same amount when cells are illuminated at an external pH 8 (corresponding to the conditions of our study) [4,5,7,12,38]. No such data have been reported for *Synechocystis* 6803, but it seems reasonable to expect similar values for this organism, too.

As the signals from all three 9-aminoacridine dyes

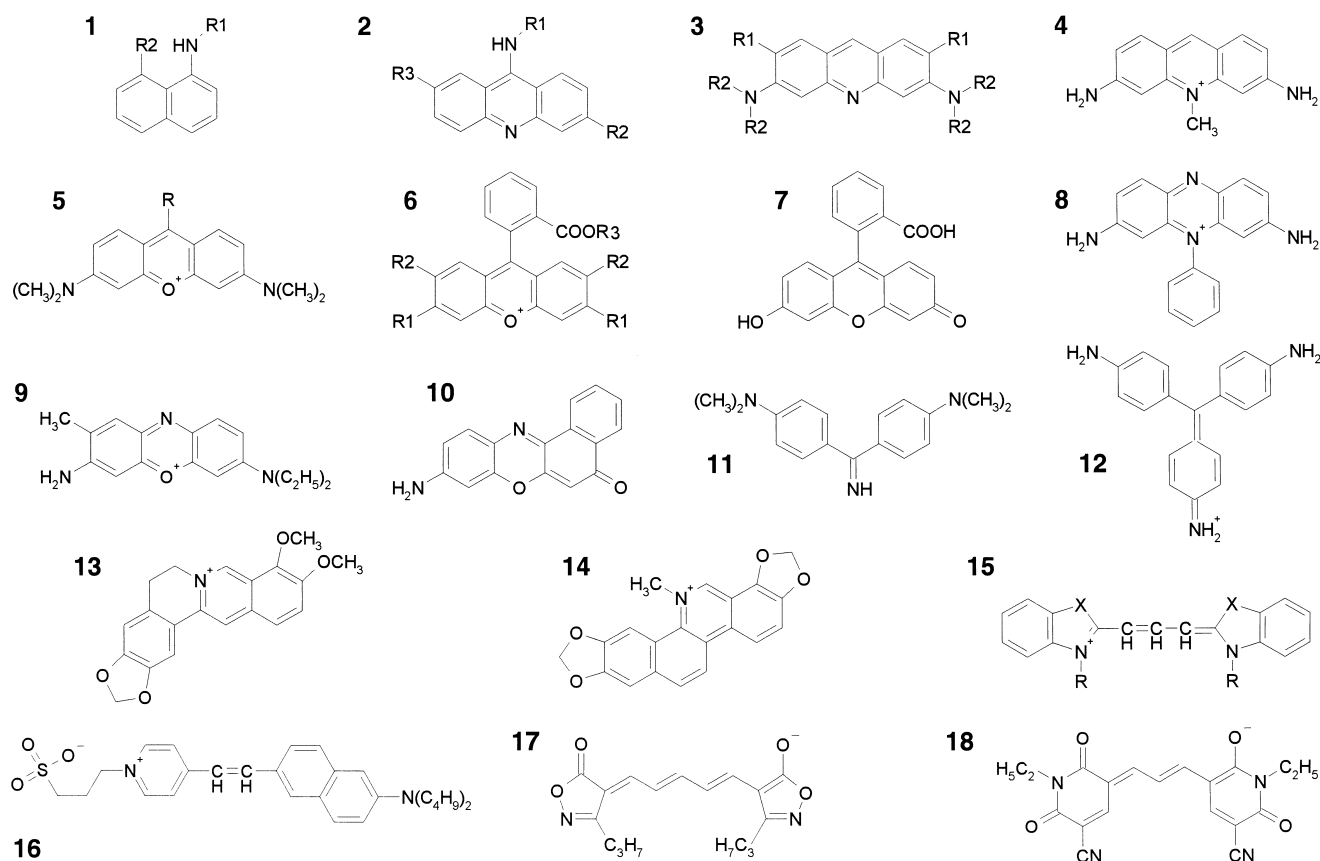


Fig. 1. Dyes used in this work. Bold numbers refer to the 'structure' column in Table 1.

were rather small, we tested additional indicators. A better signal/noise ratio was obtained with some 3,6-diaminoacridines, Proflavine and its derivatives AY and AO, which showed large signals during illumination (Fig. 2d–f). AY, which has not been used for bioenergetic measurements before, showed a large fluorescence increase during actinic illumination indicating alkalization of the cytosol (Fig. 2d). While Proflavine behaved almost identical to AY (Fig. 2e), AO [19] showed several kinetic phases (Fig. 2f): A fast decrease of fluorescence in the light indicated the acidification of the lumen; this was followed by a slower increase indicating alkalization of the cytosol, which probably lagged behind due to its dependence on the energy equivalents produced in the light. When the illumination was turned off, a fast increase of indicator fluorescence indicated the collapse of the ΔpH across the thylakoid membrane. Finally the signal declined slowly (half time of several minutes) towards the initial fluorescence, indicating a slow

de-energization of the cytosol as energy equivalents were used up. The AO signals were similar to those obtained with QA, but more pronounced. As expected for ΔpH -dependent signals, the changes of AY and AO fluorescence could be suppressed by protonophoric uncouplers such as CCCP at concentrations of 100 μM (not shown). In contrast, the fluorescence of the cationic Acriflavine did not change during illumination (Fig. 2g). This corresponds to the behavior of the positively charged 10-*N*-Nonyl Acridine orange, which binds to mitochondrial membranes without responding to membrane energization [39]. Rivanol, a 6,9-diaminoacridine with a lower $\text{p}K_a$ than the other acridines (5.8 vs. 9...11), also showed no light-induced signals (not shown).

Uptake into the cells was followed by monitoring dye fluorescence in the dark. The tendency of the various acridines to show light-induced fluorescence changes correlated with the kinetics of dye uptake

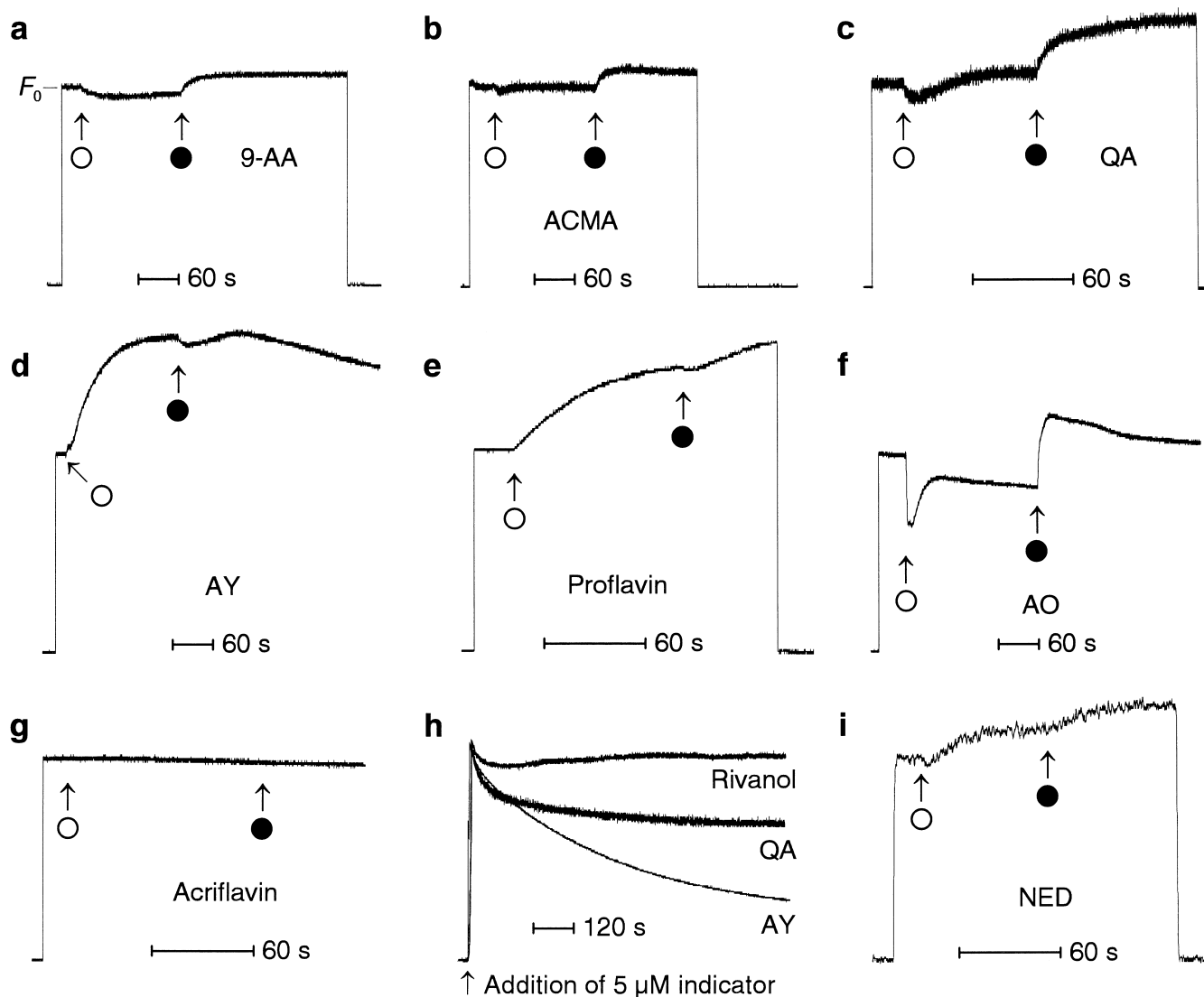


Fig. 2. Screening of ΔpH indicators as indicated with whole cells of *Synechocystis* 6803 WT by illumination with saturating RL (O, light on; ●, light off) (a–g,i). F_0 is the 100% level of indicator fluorescence before actinic illumination, as shown in a. In h the kinetics of dye uptake in the dark was monitored. Wavelengths for excitation and emission of dye fluorescence according to Table 1; NED was excited at 360 nm. Indicator concentration was 10 μM for Acriflavin and NED, 20 μM for Rivanol and 5 μM for all other dyes.

(Fig. 2h): Rivanol did not significantly accumulate in the cells, while the fluorescence of AY decreased considerably during dark incubation.

In addition to the acridines we tested NED, which is a good ΔpH indicator for isolated thylakoids from higher plants [24]. It showed a fluorescence increase in the light, followed by another small increase during the subsequent dark period (Fig. 2i). However, the signal/noise ratio was low due to the unfavorable short wavelengths for excitation and emission of this

indicator. Another disadvantage was the high background fluorescence of the cells at these wavelengths: About 75% of the F_0 level shown in Fig. 2i was autofluorescence.

All pH indicators presented so far are distributive dyes, which diffuse across membranes and undergo redistribution between the different compartments, dependent on local pH changes. An alternative method is the use of in situ dyes, which are trapped in a specific compartment to selectively indicate the pH

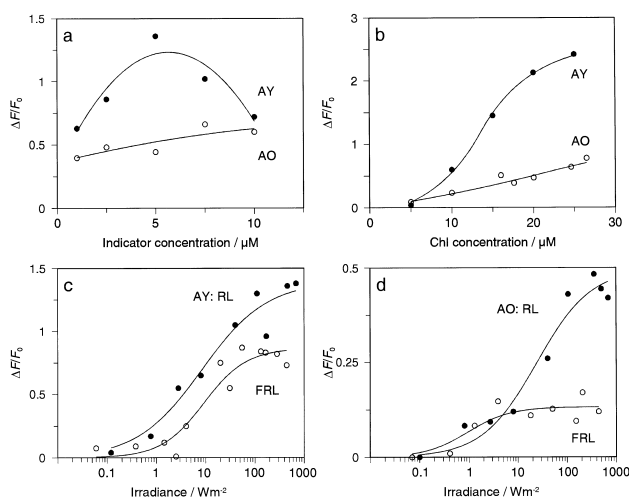


Fig. 3. Characterization of light-induced fluorescence changes of the ΔpH indicators Acridine yellow and Acridine orange in dependence of indicator concentration (a), chlorophyll *a* concentration (b) or irradiance (c,d), respectively. Chlorophyll *a* concentration in a,c,d was about 15 μM ; indicator concentration in b–d was 5 μM ; irradiance in a,b was 500 W m^{-2} . For the AY signal the dark–light transition was used, for the AO signal the light–dark transition was used (see Fig. 2d,f).

changes there. As a representative of such dyes we used FDA, the nonfluorescent diacetate of Fluorescein. After diffusion into the cytosol, the diacetate is hydrolyzed by esterases and the trapped free dye can monitor local pH changes. This method was introduced for yeast cells [40] and it has also been used successfully for some cyanobacterial cells [22]; however, with *Synechocystis* 6803, uptake and/or intracellular hydrolysis of FDA were slow: even at elevated temperature (40°C) and a high starting concentration of the dye (80 μM), only a few percent of FDA were hydrolyzed after 1 h and no light-induced fluorescence changes were detectable (not shown).

Among the various dyes tested here, AY and AO emerged as the most promising pH indicators and were therefore characterized in more detail (Fig. 3). For AY, the fluorescence change between the dark state and the steady state level during illumination was used as an indication of the alkalization of the cytosol. In the case of AO, we used instead the fast fluorescence increase at the end of the illumination, reflecting the acidification of the thylakoid lumen. Both dyes showed a concentration dependence of the signal, although in a different way (Fig. 3a): While the AO fluorescence increased with increasing

concentration, the AY fluorescence showed a marked maximum at 5 μM . Such a dependence of $\Delta F/F_0$ on the total indicator concentration indicates a dimerization, which in turn prevents a simple calculation of ΔpH from $\Delta F/F_0$ (see Section 2.4).

Upon variation of the chlorophyll concentration (Fig. 3b), the AY signal reached saturation above approximately 20 μM Chl, similar to the behavior of 9-AA with isolated thylakoids [17]. For AO, in contrast, no saturation was reached up to 25 μM Chl. We also investigated the dependence of the signals on the intensity of the actinic red or far red light (Fig. 3c,d). For both dyes, in particular for AO, the signals under far red illumination were substantially smaller than under red illumination.

3.2. AY as indicator for investigating whole-cell bioenergetics in *Synechocystis* 6803

Fig. 4 shows schematically the cellular bioenergetics of *Synechocystis* 6803. To distinguish between the different processes, we used the fluorescence increase of AY as indication of the energization of the cytoplasmic membrane by ATP and/or NADPH, which are generated at the thylakoid membrane during illumination. The following parameters have been varied:

1. Illumination either by RL (excites both photosystems) or by FRL (excites PS I only)
2. Various inhibitors of the different protein complexes have been applied
3. Deletion strains lacking one or more of the following proteins have been used: $\Delta\text{PS I}$ [32], $\Delta\text{PS II}$ [33], M55 (NDH-1 deleted) [36], $3\times\Delta\text{Ox}$ (all terminal respiratory oxidases deleted) [34] and $3\times\Delta\text{Ox}\Delta\text{PS II}$ (C.A. Howitt, W.F.J. Vermaas, personal communication)

3.2.1. Role of PS I in linear and cyclic electron transport

During RL illumination, only small signals were observed with $\Delta\text{PS I}$ cells (Fig. 5a) or WT cells in the presence of the PS I-inhibitor DSPD (Table 2). With both linear and cyclic photosynthetic electron transport being dependent on PS I, this residual activity in the absence of a functional PS I should involve PS II, probably as a short-circuited electron

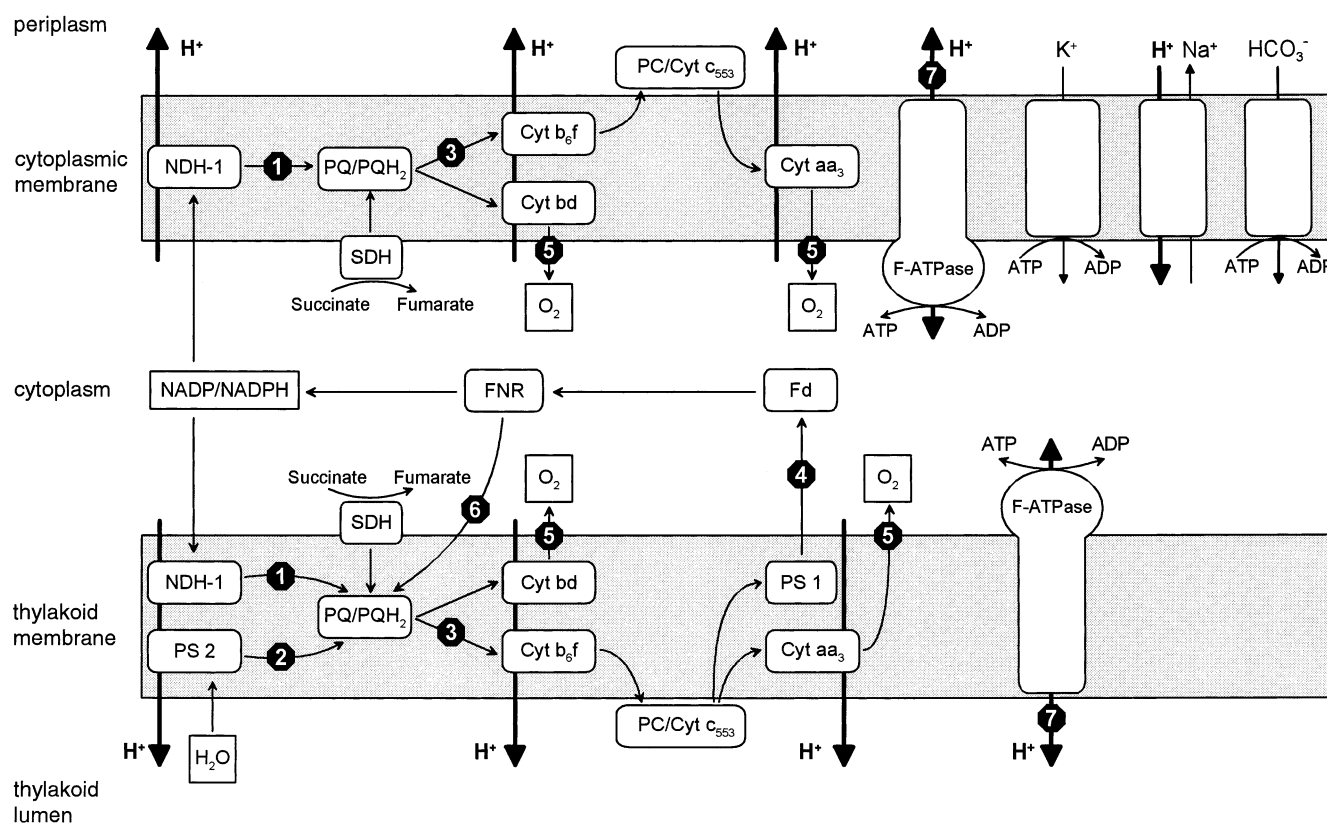


Fig. 4. Overall model of cellular energetics in *Synechocystis* 6803. The stop signs indicate the possible sites of action of (1) rotenone and TTFA, (2) DCMU and atrazine, (3) DBMIB, (4) Fecy, MV and DSPD, (5) NaN₃ and KCN, (6) antimycin A, (7) DCCD.

transport from water to the terminal oxidases, which is confirmed by DCMU sensitivity (Fig. 5b). Considering an electron transport capacity of the oxidases of about 10% relative to photosynthetic electron transport [41,42], only small signals could be expected with cells lacking a functional PS I. Also, inhibition of the cytochrome *b*₆f complex, which is located in the central part of both linear and cyclic electron transport, by DBMIB showed strongly declining signals (Table 2).

3.2.2. Effects of the PS I acceptor MV

By accepting electrons from PS I, MV supports linear and inhibits cyclic electron transport. Under conditions of an active PS II (RL, both WT and 3×ΔOx mutant), signals increased in the presence of MV (Table 2), but not when PS II was inactive (WT+FRL or a PS II-less mutant+RL). This indicates a limitation of the linear electron transport at the acceptor side of PS II and/or PS I, which was

overcome by MV. In line with this interpretation, another PS I acceptor, Fecy, showed similar effects, though at a lower level (Table 2).

3.2.3. PS II activity and the redox poise of the plastoquinone pool

Fig. 3c had shown that the AY signals of WT cells under far red light correspond to about 65% of those under red light. Likewise, in WT and 3×ΔOx cells, signals in the presence of saturating concentrations of the PS II inhibitors DCMU or atrazine are at 50–70% of the control (Table 2); these inhibitors showed no effect in the PS II-less strains ΔPS II (not shown) and 3×ΔOxΔPS II (Table 2), confirming a specific action at PS II. According to these results, the PS I cycle alone contributes to a substantial ΔpH across the cytoplasmic membrane via the production of ATP. However, permanent deletion of PS II resulted in a considerable signal decrease, the fluorescence changes were only $\Delta F/F_0 = 0.07 \pm 0.04$ (4) (RL) and

0.13 ± 0.05 (3) (FRL) in the Δ PS II strain (Fig. 5c,d). This could imply an increased rate of respiration in the Δ PS II strain, rendering the cytosol more alkaline in the dark and thus diminishing the light-induced pH-change. However, this cannot be the sole explanation, since similarly small signals of $\Delta F/F_0 = 0.33 \pm 0.15$ (5) (RL) and 0.31 ± 0.08 (3) (FRL) were also observed in the $3 \times \Delta$ Ox Δ PS II strain (not shown), which does not respire. Therefore, an unexplained discrepancy remains comparing the experiments with inhibition and complete deletion of PS II, respectively; we can only speculate that some critical requirement for optimum function of the PS I cycle, such as the redox poise of the electron transport chain, is affected in PS II-less strains.

3.2.4. Participation of NDH-1 in the PS I cycle

Using the NDH-1-less M55 mutant, we observed a signal of about 50% of the WT control under RL illumination (Fig. 5e); this indicates the ability of linear electron transport at the thylakoid membrane to support the formation of a substantial Δ pH at the CM. On the other hand, almost no fluorescence change of AY occurred during FRL illumination of M55 cells (Fig. 5f); this is in accordance with NDH-1 participating in PS I cyclic electron flow in *Synechocystis* 6803 [43,44]. Values for $\Delta F/F_0$ of 50...70% of the control have also been observed when WT cells were illuminated with RL in the presence of saturating concentrations of antimycin A [45] or TTFA [46] to inhibit cyclic electron transport (Table 2). How-

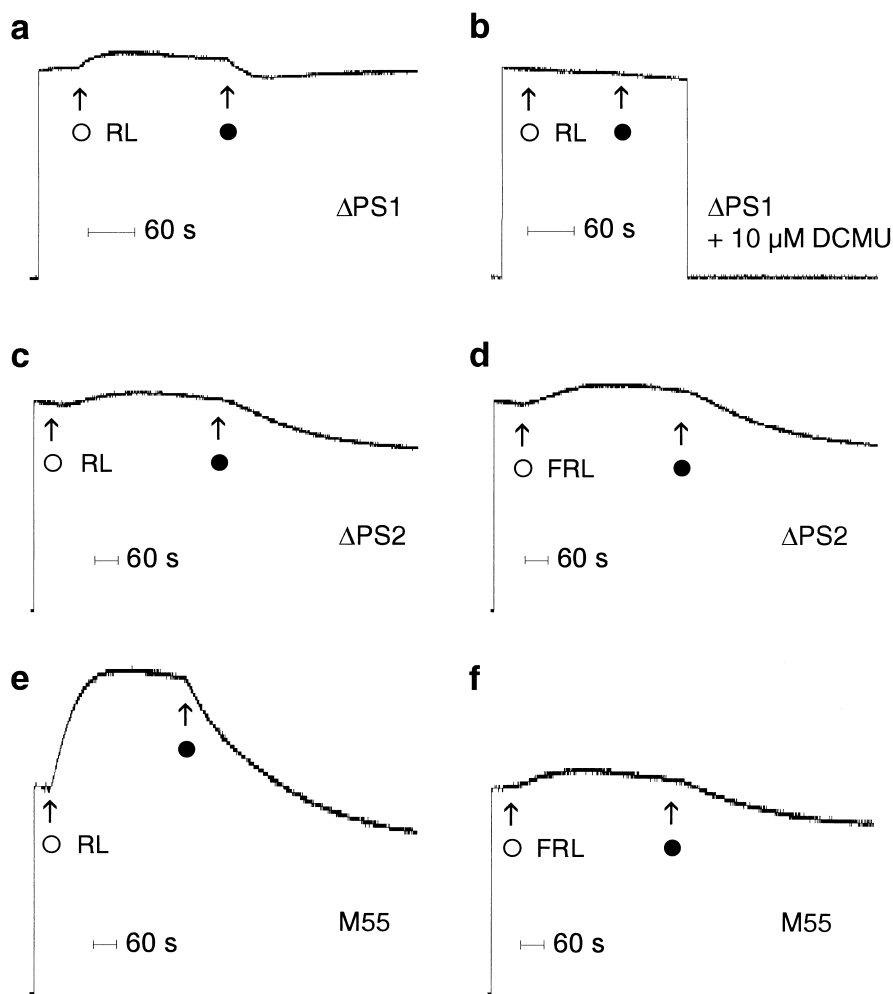


Fig. 5. Fluorescence changes of the Δ pH indicator Acridine yellow upon illumination of the *Synechocystis* 6803 mutant strains Δ PS I (a,b), Δ PS II (c,d) and M55 (e,f) with saturating RL or FRL, as indicated (○, light on; ●, light off). Cells were adjusted to approximately equal cell density (measured as OD at 750 nm), corresponding to 15 μ M Chl in WT cells.

Table 2

Effects of various inhibitors and artificial electron acceptors on the fluorescence change of AY induced by saturating illumination of *Synechocystis* 6803 WT, oxidase-less and oxidase-less/PS II-less strains

Compound	Signal/% of control			
	WT Red light	WT Far red light	3×ΔOx Red light	3×ΔOxΔPS II Red light
2 mM DSPD	22	8		26 ± 7 (2)
50 μM DBMIB	17 ± 17 (4)	0	4	37 ± 4 (3)
200 μM MV	146 ± 44 (7)	105 ± 9 (4)	131 ± 13 (2)	83 ± 8 (5)
1 mM Fecy	104 ± 3 (2)		110 ± 1 (2)	79 ± 17 (2)
10 μM DCMU	50 ± 27 (5)		63	103 ± 19 (3)
20 μM Atrazine	74 ± 10 (5)			
10 μM TTFA	53 ± 6 (3)	46 ± 13 (3)		
50 μM Antimycin A	67 ± 14 (2)	47 ± 9 (3)	80	86 ± 8 (3)
100 μM Rotenone	99 ± 1 (2)	90 ± 0 (3)	74	91
5 mM KCN	126 ± 14 (7)			
1 mM NaN ₃	109 ± 11 (3)	88 ± 18 (2)		
2.5 mM DCCD	86 ± 14 (5)		0 ± 0 (3)	
2.5 mM DCCD+5 mM KCN	22 ± 31 (3)			

Values without standard deviation are from single determinations.

ever, no complete inhibition of the PS I cycle was achieved with antimycin A or TTFA in WT cells: small signals are still detectable under FRL illumination (Table 2). This may indicate an alternative PS I cycle in cyanobacteria [47,48], independent of NDH-1 and possibly involving the FNR. TTFA has been reported to inhibit NDH-1 in *Synechocystis* 6803, while antimycin A acts at another site [43]. Rotenone, which inhibits NDH-1 in isolated thylakoid membranes of *Synechocystis* 6803 [43], showed no effect with whole cells (Table 2).

3.2.5. Respiration and ATP hydrolysis at the cytoplasmic membrane

The 3×ΔOx strain lacking all three respiratory terminal oxidases [34] showed a red light-induced $\Delta F/F_0$ of 1.39 ± 0.39 (18) (not shown), which is most probably induced by ATP hydrolysis and which is comparable in size to the WT signal (see Fig. 3c). The fact that KCN and NaN₃ showed no inhibition in WT cells (Table 2) also implicates that respiration is not obligatory for cytoplasmic membrane energization. As *Synechocystis* 6803 contains no P-type H⁺-ATPase [29], an F-type ATPase should be responsible for the ATP-dependent proton extrusion. Indeed, the F-type ATPase inhibitor DCCD completely suppressed the alkalization of the cytosol in the 3×ΔOx mutant (Table 2), whereas it showed almost no effect in WT cells (Table 2); however, in combination with

KCN, DCCD showed a strong inhibition. These findings indicate that either NADPH or ATP alone could induce light-driven proton extrusion in *Synechocystis* 6803, which can only be blocked by a complete inhibition of both respiration and ATP hydrolysis at the same time.

3.3. Transport processes at the cytoplasmic membrane of *Synechocystis* 6803

As shown in Fig. 4, various energy dependent transport processes at the CM of cyanobacteria – such as uptake of K⁺, extrusion of Na⁺ and uptake of inorganic carbon – interact with photosynthetic energy generation. Therefore, we used the ΔpH indicators AY and AO to study transport processes and osmotic regulation (Fig. 6).

The fluorescence of AY decreases immediately when *Synechocystis* 6803 cells are osmotically shocked by addition of 550 mM NaCl (Fig. 6a), KCl (Fig. 6b), betaine (Fig. 6c) or glycerol (Fig. 6d). It has been reported that cyanobacterial cells rapidly shrink after an increase of extracellular osmolarity [19,49], and we interpret the fast fluorescence decrease after solute addition as a reflection of this process. In the case of NaCl, the signal recovered within a few minutes (Fig. 6a); this correlates to the osmotic stabilization by means of sodium uptake, which is the second phase of adaptation to NaCl

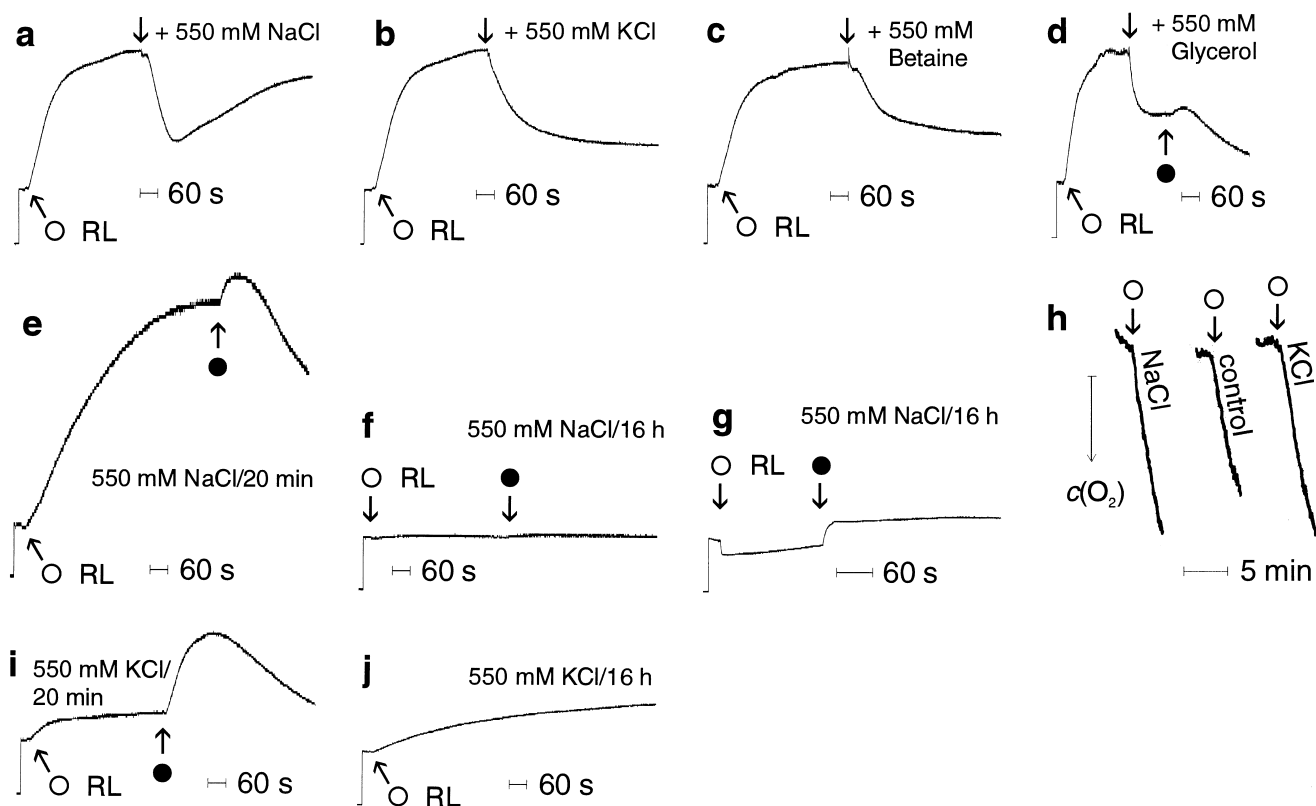


Fig. 6. Effects of osmotic shock and transport processes across the cytoplasmic membrane in *Synechocystis* 6803 WT cells. (a–d) Fluorescence changes of Acridine yellow during saturating RL illumination, induced by addition of 550 mM NaCl (a), 550 mM KCl (b), 550 mM betaine (c) and 550 mM glycerol (d). (e,f) Light-induced fluorescence changes of Acridine yellow after 20 min (e) or 16 h incubation (f) with 550 mM NaCl. (g) Light-induced fluorescence change of Acridine orange after 16 h incubation with 550 mM NaCl. (h) Oxygen evolution during saturating RL illumination of salt adapted (550 mM NaCl or KCl, 16 h) and control cells in the presence of 10 mM NaHCO_3 . (i,j) Light-induced fluorescence changes of Acridine yellow after 20 min (i) or 16 h incubation (j) with 550 mM KCl. (O), light on; (●), light off.

stress in cyanobacteria after the initial shrinking [19,49]. This process has been reported to be specific for NaCl, and, accordingly, was not observed with the other solutes (Fig. 6b–d). After 20 min incubation with 550 mM NaCl (Fig. 6e), the light-induced $\Delta F/F_0$ was strongly increased compared to control cells (the same effect was observed after 20 min NaCl incubation of $\Delta\text{PS II}$ cells, not shown), corresponding to the increase of photosynthetic capacity, in particular of cyclic electron transport, in salt-stressed *Synechocystis* 6803 cells to meet the energy requirements of salt adaptation [44,47,48].

After 16 h incubation with 550 mM NaCl, there was surprisingly almost no change of AY fluorescence during illumination (Fig. 6f); using AO a signal was still detectable, but indicated only luminal acidification (Fig. 6g). Besides this, the cells seemed

unimpaired: the rate of photosynthetic oxygen evolution was identical for control and salt adapted cells after 16 h (Fig. 6h) and, according to fluorescence emission spectra recorded at 77 K, there were no differences in the photosystem stoichiometry between the differently pretreated cultures (not shown). The absence of signals of CM energization for both indicators in Fig. 6f,g probably indicated an increased rate of Na^+/H^+ exchange: A high Na^+/H^+ antiporter activity at high sodium concentration may act like a protonophoric uncoupler of the CM, eliminating the indicator signal of cytosolic pH changes. Evidence supporting this hypothesis is the partial recovery of the AY signal upon decreasing the external Na^+ concentration by washing salt-adapted cells with normal BG-11 medium containing a low concentration of Na^+ (not shown).

In contrast to the mechanisms enabling adaptation to NaCl stress, there are obviously no comparable mechanisms for KCl: The light-induced $\Delta F/F_0$ of AY after incubation with 550 mM KCl for 20 min (Fig. 6i) or 16 h (Fig. 6j) was considerably lower than in control cells.

3.4. Screening of $\Delta\Psi$ indicators in *Synechocystis* 6803

Many $\Delta\Psi$ indicators, which are useful in pigment-free systems such as mitochondria or neurons, are less suited for whole cyanobacterial cells and we therefore tested a range of candidate dyes. The xanthenes R123, R6G, TMRM, Pyronin G and TMROS [2,50,51] were readily transported into the cells (Fig. 7a,b). This process was dependent on respiratory membrane energization, since it was abolished by the addition of CCCP (Fig. 7b) or KCN (not shown). All xanthenes showed fluorescence changes during illumination, as demonstrated for R6G (Fig. 7c), but the signals had large irreversible components, which probably indicate metabolization of the dyes, like the well-known reductive bleaching of phthaleins [52]. While the azine Phenosafranin [53] did not yield light-induced signals (not shown), the oxazine BCB showed a 10% decrease of F_0 (Fig. 7d). BCB has not yet been discussed as a $\Delta\Psi$ indicator, but it is structurally similar to xanthenes and azines. In contrast, the uncharged oxazine Nile Red did not yield such signals (not shown). The fast kinetics of the BCB signal may indicate that it monitors preferentially the thylakoid membrane, as the potential at this membrane should respond quickly upon light on and off. However, the emission maximum of 650 nm complicates the use of BCB for investigations in phycobilisome-containing strains. The carbocyanine dyes DiIC18(3) and DiSC8(3) [54] showed only weak fluorescence in the presence of cells; a large irreversible component of the fluorescence change occurred with DiOC2(3) (Fig. 7e). Negative results were also obtained with the isoquinolinium alkaloids Berberine [55] and Sanguinarine, with the basic arylmethane dyes Auramine O and Fuchsin [15], and with Oxonol VI and Oxonol 595 [18,21] (not shown). ANS and Di-4-ANEPPS accumulate in the outer membrane leaflet of cytoplasmic membranes, where they selectively monitor $\Delta\Psi$ changes. ANS showed a fluorescence increase upon alteration of the CM surface

potential by addition of KCl (Fig. 7f), as reported earlier for *Anacystis nidulans* [10]. This is no nonspecific effect of ionic strength, since without cells a fluorescence change of opposite sign occurred (Fig. 7g). We could, however, not observe light-induced changes of ANS fluorescence (not shown). In contrast, Di-4-ANEPPS shows a $\Delta F/F_0$ of about 3% upon illumination (Fig. 7h), which would correspond to a potential decrease of -30 mV [56]. However, with respect to the unexplained continuation of fluorescence changes of this dye after illumination, this result should be treated with caution.

Apart from all biochemical and spectroscopic difficulties with the $\Delta\Psi$ indicators, it seems likely that the light-induced $\Delta\Psi$ changes at the CM are small: -30 mV as estimated from our measurements with Di-4-ANEPPS in *Synechocystis* 6803 are comparable with data reported for other cyanobacteria [5,6,57]. At the thylakoid membrane only small changes in the range of 10 mV, similar to values published for higher plant thylakoids [58–60], would be expected.

3.5. Comparative measurements with *Synechococcus elongatus*

Some measurements have been performed with the thermophilic cyanobacterium *Synechococcus elongatus* to check whether the results obtained with bioenergetic indicators for *Synechocystis* are valid also for this organism. The ΔpH indicators ACMA and NED yielded only small signals (about 10% fluorescence change), comparable to the results with *Synechocystis* 6803 (see above). AY and AO, which turned out to be the best in the studies with *Synechocystis* 6803, also yielded similar signals with *S. elongatus*, although in the case of AO a higher Chl concentration of about 70 μM was required to produce signals of the shape observed with *Synechocystis* 6803 already at 15 μM Chl. $\Delta\Psi$ indicators like ANS, Pyronin G and TMROS showed no light-induced fluorescence changes in *S. elongatus*.

However, despite the similarities between the two species, there was one major difference: while in *Synechocystis* 6803 WT cells the AY signals under far red light were substantially smaller than under red light, the FRL signals in *S. elongatus* were higher than the RL signals: $\Delta F/F_0 = 0.29 \pm 0.13$ (5) (RL); $\Delta F/F_0 = 0.40 \pm 0.16$ (5) (FRL). An explanation for

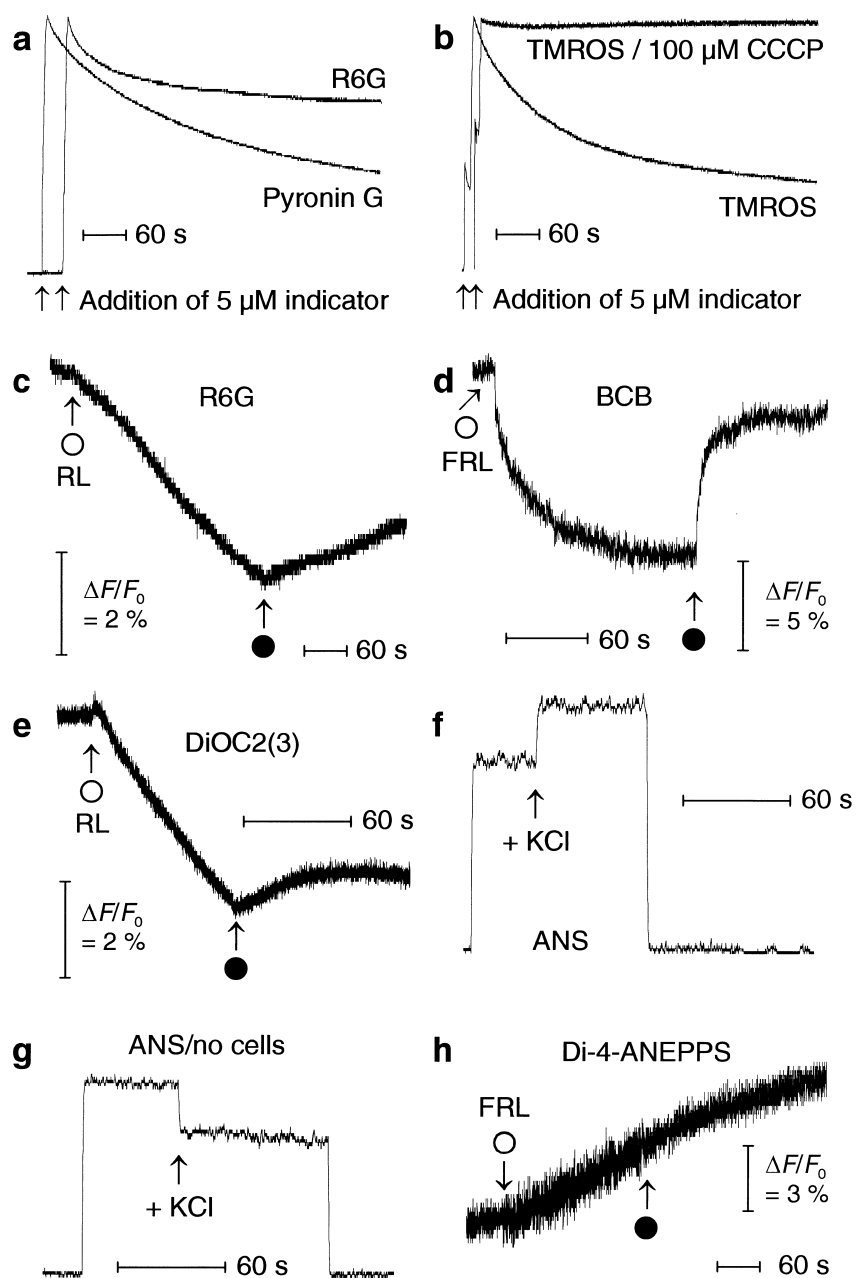


Fig. 7. Screening of various $\Delta\Psi$ indicators with whole cells of *Synechocystis* 6803 WT (a–c, e–h) and the PAL mutant (d). (a,b) Kinetics of dye uptake in the dark for R6G and Pyronin G (a) and TMROS (b). (c–e) Fluorescence changes of R6G (c), BCB (d) and DiOC2(3) (e), induced by illumination with saturating red or far red light as indicated (○, light on; ●, light off). (f,g) Fluorescence change of ANS induced by addition of 100 mM KCl in the dark in the presence (f) or absence (g) of cells. (h) Fluorescence change of Di-4-ANEPPS induced by illumination with saturating far red light. Indicator concentration was 10 μM , except for e and h where 5 μM DiOC2(3) and 50 μM Di-4-ANEPPS have been used, respectively.

this discrepancy could be a preferential energization of the CM in *S. elongatus* by ATP hydrolysis, which is supported by far red light favoring the PS I cycle. This view is supported by the complete suppression

of cytosolic alkalization in the presence of the F-type ATPase inhibitor DCCD, which had only a marginal effect in *Synechocystis* 6803 (compare Table 2). In general, the contribution of NADPH oxidation and

ATP hydrolysis for the ΔpH generation across the CM varies between different cyanobacterial species [8,11]: While energization mainly by ATP has been reported for *Anabaena variabilis* [61,62], respiration was reported to be the major energy source in *Anacystis nidulans* [10,22] and *Plectonema boryanum* [63] (but see also [27]). Our results indicate that the fluorescence dyes found in this study can be a valuable tool to elucidate the much less characterized bioenergetics of *S. elongatus*.

4. Summary

(1) The acridine dyes Acridine orange and Acridine yellow are useful ΔpH indicators for measurements with whole cells of *Synechocystis* 6803 and *Synechococcus elongatus*. They can be used complementarily, since AY exclusively monitors the cytosol, while AO responds to pH changes in both the cytosol and the lumen. AY may be especially useful for the investigation of the cyclic electron transport, complementing established methods like the kinetics of P700^+ and photoacoustic measurements. With these dyes, the interplay of various cellular bioenergetic processes (see Fig. 4) can be monitored.

(2) Production of energy equivalents for energization of the cytoplasmic membrane in *Synechocystis* 6803 is possible either by linear or by cyclic photosynthetic electron transport alone. However, for optimum yield both pathways have to cooperate.

(3) The energy provided by the photosynthetic light reactions can be utilized at the cytoplasmic membrane of *Synechocystis* 6803 either by NADPH oxidation or by ATP hydrolysis; both pathways can replace each other. In contrast, proton extrusion at the cytoplasmic membrane of *S. elongatus* is driven exclusively by ATP hydrolysis.

(4) AY can also be used to study osmotic regulation; during adaptation to salt stress, different phases in the response of *Synechocystis* 6803 can be distinguished.

(5) The $\Delta\Psi$ indicator Di-4-ANEPPS shows a light-induced fluorescence change, which probably indicates a -30 mV decrease of the cytoplasmic membrane potential of *Synechocystis* 6803. This is complemented by the oxazine dye BCB, which shows a transient fluorescence decrease upon illumination,

tentatively assigned to a change of $\Delta\Psi$ at the thylakoid membrane.

Acknowledgements

The authors would like to thank Drs Wim Vermaas (Tempe, Arizona), Teruo Ogawa (Nagoya, Japan) and Ghada Ajlani (Grenoble, France) for providing the mutant strains used in this study, and our late colleague Klaus Masson (Bochum) for the separation of Proflavine/Acriflavine. This work was supported by the Deutsche Forschungsgemeinschaft (SFB 480/TP C1).

References

- [1] J.C. Smith, Biochim. Biophys. Acta 1016 (1990) 1–28.
- [2] R.P. Haugland, Molecular Probes. Handbook of Fluorescent Probes and Research Chemicals, Molecular Probes Inc., Eugene, OR, 1992.
- [3] W.T. Mason, Fluorescent and Luminescent Probes for Biological Activity, Academic Press, San Diego, CA, 1999.
- [4] G. Falkner, F. Horner, K. Werdan, H.W. Heldt, Plant Physiol. 58 (1976) 717–718.
- [5] E. Padan, S. Schuldiner, J. Biol. Chem. 253 (1978) 3281–3286.
- [6] R.H. Reed, P. Rowell, W.D.P. Stewart, Eur. J. Biochem. 116 (1981) 323–330.
- [7] J. Gibson, Arch. Microbiol. 130 (1981) 175–179.
- [8] A.E. Walsby, in: N.G. Carr, B.A. Whitton (Eds.), The Biology of Cyanobacteria, Blackwell Scientific Publications, 1982, pp. 237–262.
- [9] R. Muchl, G.A. Peschek, Curr. Microbiol. 11 (1984) 179–182.
- [10] G.A. Peschek, T. Czerny, G. Schmetterer, W.H. Nitschmann, Plant Physiol. 79 (1985) 278–284.
- [11] G.A. Peschek, W.H. Nitschmann, T. Czerny, Methods Enzymol. 167 (1988) 361–379.
- [12] S. Belkin, R.J. Mehlhorn, L. Packer, Plant Physiol. 84 (1987) 25–30.
- [13] M. Kneen, J. Farinas, Y. Li, A.S. Verkman, Biophys. J. 74 (1998) 1591–1599.
- [14] R. Kraayenhof, FEBS Lett. 6 (1970) 161–165.
- [15] M. Nishimura, in: B. Chance, L. Chuan-pu, J.K. Blasie (Eds.), Probes of Structure and Function of Macromolecules and Membranes, Vol. I, Probes and Membrane Function, Academic Press, New York, 1971, pp. 227–233.
- [16] S. Schuldiner, H. Rottenberg, M. Avron, Eur. J. Biochem. 25 (1972) 64–70.
- [17] J.W. Fiolet, E.P. Bakker, K. van Dam, Biochim. Biophys. Acta 368 (1974) 432–445.

- [18] J.J. Schuurmans, R.P. Casey, R. Kraayenhof, *FEBS Lett.* 94 (1978) 405–409.
- [19] E. Blumwald, J.M. Wolosin, L. Packer, *Biochem. Biophys. Res. Commun.* 122 (1984) 452–459.
- [20] H.J. Lubberding, J. Schroten, *Photosynth. Res.* 7 (1986) 247–256.
- [21] K. Krab, E.J. Hotting, H.S. van Walraven, M.J.C. Scholts, R. Kraayenhof, *Bioelectrochem. Bioenerg.* 16 (1986) 55–62.
- [22] B. Hinterstoisser, G.A. Peschek, *FEBS Lett.* 217 (1987) 169–173.
- [23] T. Vu-Van, T. Heinze, J. Buchholz, B. Rumberg, in: J. Biggins (Ed.), *Progress in Photosynthesis Research*, Vol. III, Martinus Nijhoff, Dordrecht, 1987, pp. 189–192.
- [24] B. Rumberg, K. Schubert, F. Strelow, T. Tran-Anh, in: M. Baltscheffsky (Ed.), *Current Research in Photosynthesis*, Vol. III, Kluwer Academic Publishers, 1990, pp. 125–128.
- [25] E.L. Barsky, M.V. Gusev, K.A. Nikitina, V.D. Samuilov, *Arch. Microbiol.* 129 (1981) 105–108.
- [26] I.I. Severina, V.P. Skulachev, *FEBS Lett.* 165 (1984) 67–71.
- [27] H.C.P. Matthijs, J.M. van Steenbergen, R. Kraayenhof, *Photosynth. Res.* 7 (1985) 59–67.
- [28] P.K. Mohapatra, H. Schubert, U. Schiewer, *Bull. Environ. Contam. Toxicol.* 57 (1996) 722–728.
- [29] T. Kaneko, S. Sato, H. Kotani, A. Tanaka, E. Asamizu, Y. Nakamura, N. Miyajima, M. Hirose, M. Sugiura, S. Sasamoto, T. Kimura, T. Hosouchi, A. Matsuno, A. Muraki, N. Nakazaki, K. Naruo, S. Okumura, C. Takeuchi, T. Wada, A. Watanabe, M. Yamada, M. Yasuda, S. Tabata, *DNA Res.* 3 (1996) 109–136.
- [30] N. Krauss, W. Hinrichs, I. Witt, P. Fromme, W. Pritzkow, Z. Dauter, C. Betzel, K.S. Wilson, H.T. Witt, W. Saenger, *Nature* 361 (1993) 326–331.
- [31] H. Kuhl, J. Kruip, A. Seidler, A. Krieger-Liszkay, M. Bünker, D. Bald, A.J. Scheidig, M. Rögner, *J. Biol. Chem.* 275 (2000) 20652–20659.
- [32] G. Shen, S. Boussiba, W.F.J. Vermaas, *Plant Cell* 5 (1993) 1853–1863.
- [33] J.J. Eaton-Rye, W.F. Vermaas, *Plant Mol. Biol.* 17 (1991) 1165–1177.
- [34] C.A. Howitt, W.F.J. Vermaas, *Biochemistry* 37 (1998) 17944–17951.
- [35] G. Ajlani, C. Vernotte, *Plant Mol. Biol.* 37 (1998) 577–580.
- [36] T. Ogawa, *Proc. Natl. Acad. Sci. USA* 88 (1991) 4275–4279.
- [37] A.B. Hope, D.B. Matthews, *Aust. J. Plant Physiol.* 12 (1985) 9–19.
- [38] T. Kallas, F.W. Dahlquist, *Biochemistry* 20 (1981) 5900–5907.
- [39] A. Maftah, J.M. Petit, R. Julien, *FEBS Lett.* 260 (1990) 236–240.
- [40] J. Slavík, *FEBS Lett.* 140 (1982) 22–26.
- [41] G.A. Peschek, in: P. Fay, C. Van Baalen (Eds.), *The Cyanobacteria*, Elsevier, 1987, pp. 119–161.
- [42] G. Schmetterer, in: D.G. Bryant (Ed.), *The Molecular Biology of Cyanobacteria*, Kluwer Academic Publishers, Dordrecht, 1994, pp. 409–435.
- [43] H. Mi, T. Endo, T. Ogawa, K. Asada, *Plant Cell Physiol.* 36 (1995) 661–668.
- [44] Y. Tanaka, S. Katada, H. Ishikawa, T. Ogawa, T. Takabe, *Plant Cell Physiol.* 38 (1997) 1311–1318.
- [45] T. Endo, H. Mi, T. Shikanai, K. Asada, *Plant Cell Physiol.* 38 (1997) 1272–1277.
- [46] H. Mi, T. Endo, U. Schreiber, K. Asada, *Plant Cell Physiol.* 33 (1992) 1099–1105.
- [47] R. Jeanjean, S. Bédu, M. Havaux, H.C.P. Matthijs, F. Joset, *FEMS Microbiol. Lett.* 167 (1998) 131–137.
- [48] J. van Thor, R. Jeanjean, M. Havaux, K.A. Sjollem, F. Joset, K.J. Hellingwerf, H.C.P. Matthijs, *Biochim. Biophys. Acta* 1457 (2000) 129–144.
- [49] R.H. Reed, S.R.C. Warr, D.L. Richardson, D.J. Moore, W.D.P. Stewart, *FEMS Microbiol. Lett.* 28 (1985) 225–229.
- [50] B. Ehrenberg, V. Montana, M.-D. Wei, J.P. Wuskell, L.M. Loew, *Biophys. J.* 53 (1988) 785–794.
- [51] I. Tasaki, in: B. Chance, L. Chuan-pu, J.K. Blasie (Eds.), *Probes of Structure and Function of Macromolecules and Membranes*, Vol. I, Probes and Membrane Function, Academic Press, New York, 1971, pp. 235–237.
- [52] P.J. Kudirka, R.S. Nicholson, *Anal. Chem.* 44 (1972) 1786–1794.
- [53] K.E.O. Åkerman, M.K.F. Wikström, *FEBS Lett.* 68 (1976) 191–197.
- [54] A.S. Waggoner, *Methods Enzymol.* 55 (1979) 689–695.
- [55] V. Mikeš, L.S. Yaguzhinskij, *J. Bioenerget. Biomembr.* 17 (1985) 23–32.
- [56] L.M. Loew, L.B. Cohen, J. Dix, E.N. Fluhler, V. Montana, G. Salama, J.Y. Wu, *J. Membr. Biol.* 130 (1992) 1–10.
- [57] D.P. Häder, *Arch. Microbiol.* 119 (1978) 75–79.
- [58] W. Schliephake, W. Junge, H.T. Witt, *Z. Naturforsch.* 23b (1968) 1571–1578.
- [59] H.-L. Huber, B. Rumberg, U. Siggel, *Ber. Bunsenges. Phys. Chem.* 84 (1980) 1050–1055.
- [60] W. Vredenberg, A. Bulychev, H. Dassen, J. Snel, T. van Voorthuysen, *Biochim. Biophys. Acta* 1230 (1995) 77–80.
- [61] H. Paschinger, *Arch. Microbiol.* 113 (1977) 285–291.
- [62] S. Scherer, E. Stürzl, P. Böger, *J. Bacteriol.* 158 (1984) 609–614.
- [63] B. Raboy, E. Padan, *J. Biol. Chem.* 253 (1978) 3287–3291.